Biomaterials Science

ROYAL SOCIETY OF CHEMISTRY

PAPER

View Article Online
View Journal | View Issue

Cite this: *Biomater. Sci.*, 2020, **8**, 4467

Design, development, testing at ISO standards and *in vivo* feasibility study of a novel polymeric heart valve prosthesis†

Joanna R. Stasiak,[a] Marta Serrani,[a] Eugenia Biral,[a] James V. Taylor,[b] Azfar G. Zaman,[c] Samantha Jones,[d] Thomas Ness,[e] Francesco De Gaetano,[f] Maria Laura Costantino,[f] Vito D. Bruno,[g] Saadeh Suleiman,[g] Raimondo Ascione*‡[g] and Geoff D. Moggridge*‡[a]

Clinically available prosthetic heart valves are life-saving, but imperfect: mechanical valves requiring anticoagulation therapy, whilst bioprosthetic valves have limited durability. Polymer valves offer the prospect of good durability without the need for anticoagulation. We report the design and development of a polymeric heart valve, its bench-testing at ISO standards, and preliminary extra-vivo and *in vivo* short-term feasibility. Prototypes were manufactured by injection moulding of styrenic block copolymers to achieve anisotropic mechanical properties. Design was by finite element stress–strain modelling, which has been reported previously, combined with feedback from bench and surgery-based testing using various combinations of materials, valve geometry and processing conditions. Bench testing was according to ISO 5840:2015 standards using an *in vitro* cardiovascular hydrodynamic testing system and an accelerated fatigue tester. Bench comparisons were made with a best-in-class bio-prosthesis. Preliminary clinical feasibility evaluations included extra-vivo and short-term (1–24 hours) *in vivo* testing in a sheep model. The optimised final prototype met the requirements of ISO standards with hydrodynamic performance equivalent to the best-in-class bioprosthesis. Bench durability of greater than 1.2 billion cycles (30 years equivalent) was achieved (still ongoing). Extra-vivo sequential testing (n = 8) allowed refinement of external diameter, 3D shape, a low profile, flexibility, suturability, and testing of compatibility to magnetic resonance imaging and clinical sterilisation. *In vivo* short-term (1–24 hours) feasibility (n = 3) confirmed good suturability, no mechanical failure, no trans-valvular regurgitation, competitive trans-valvular gradients, and good biocompatibility at histopathology. We have developed and tested at ISO standards a novel prosthetic heart valve featuring competitive bench-based hydrodynamics and durability, well beyond the ISO requirements and comparable to a best-in-class bioprosthesis. *In vivo* short-term feasibility testing confirmed preliminary safety, functionality and biocompatibility, supporting progression to a long-term efficacy trial.

Received 13th March 2020,
Accepted 15th June 2020

DOI: 10.1039/d0bm00412j

rsc.li/biomaterials-science

[a]*Department of Chemical Engineering and Biotechnology, University of Cambridge, Cambridge, UK. E-mail: gdm14@cam.ac.uk; Tel: +44 (0)1223 334763*
[b]*Department of Engineering, University of Cambridge, Cambridge, UK*
[c]*Cardiology, Freeman Hospital and Institute of Cellular Medicine, Newcastle University, Newcastle upon Tyne, UK*
[d]*Cardiology Research, Newcastle upon Tyne NHS Hospitals Trust, Newcastle upon Tyne, UK*
[e]*Newcastle Molecular Pathology Node, Newcastle upon Tyne Hospitals NHS Hospitals Trust, Newcastle upon Tyne, UK*
[f]*Department of Chemistry, Materials and Chemical Engineering "Giulio Natta", Politecnico di Milano, Milano, Italy*
[g]*Bristol Heart Institute and Translational Biomedical Research Centre, University of Bristol, Bristol, UK. E-mail: R.Ascione@bristol.ac.uk; Tel: +44 (0)117 3423286*
†Electronic supplementary information (ESI) available. See DOI: 10.1039/d0bm00412j
‡These authors contributed equally to this work and are co-corresponding and co-senior authors.

Introduction

The search for the ideal prosthetic heart valve combining excellent durability and biocompatibility is still on. Despite the development of transcatheter devices, surgically implanted mechanical and bioprosthetic valves still represent the great majority of heart valve replacements.[1,2] Approximately 80% of surgical prostheses currently implanted are tissue valves,[3] with the use of mechanical valves gradually declining.

The usual lifespan of bioprosthetic valves is 10–15 years. While they feature good biocompatibility and no need for anticoagulation, their risk of structural deterioration is an issue, particularly in young patients or due to exacerbated calcification.[4,5] Mechanical valves have excellent durability,

but require anticoagulation, causing significant haemorrhagic or thromboembolic risks, resulting from the thrombogenicity of materials and high shear stresses, particularly around the hinge points, which damages blood and activates clotting.[6]

Polymeric heart valves (PHVs) are predominantly constructed of polymer-based materials which have good biocompatibility and biostability.[7] They may combine the advantages of mechanical and bioprosthetic valves, hence with potential to impact on patient wellbeing. Unlike the laborious hand sewing of biological tissue onto frames, PHVs can be manufactured using simple and automated fabrication techniques and can therefore be significantly less expensive and with better quality control. There has been a substantial work in recent years to develop a PHV[7,8] but none has yet reached the clinic, although recently the Foldax Tria surgical polymeric valve (https://foldax.com/) has undergone first-in-human implantation, with no data published yet. As well as valves for surgical implantation which is the topic of this paper, polymeric leaflets also show promise for trans-catheter valves.[9,10]

Styrenic triblock copolymers (STCPs) are synthetic thermoplastic elastomers amenable to high-throughput injection moulding, with applications in medicine, for example in a commercial drug-eluting coronary stent.[11] They contain polystyrene hard domains in a continuous elastomeric phase; with the hard domains forming physical cross-links and providing strength, while the elastomeric phase gives flexibility and elasticity. Altering the relative fraction of hard and soft segments results in a range of morphologies at the nano-scale, driven by the immiscibility of the different blocks. Thus by selecting different block copolymers with specific molecular weights and styrene fractions[12] it is possible to manufacture a whole 3D dynamic PHV, featuring two or more levels of flexibility in stent and leaflet areas. In addition, STCPs with a styrene content in the range 20–33% self assemble into cylindrical microstructure; and hot melt processing of such STCPs with cylindrical microstructure can produce structural anisotropy, with different mechanical properties in two orthogonal directions,[13–15] mimicking the mechanics of native heart valve tissue.[16,17] Finite element modelling has shown that, if correctly distributed within a heart valve leaflet, such anisotropy substantially reduces the peak strain energy density the material is exposed to and so may enhance durability.[18] Previous publications explain how such a desirable distribution of anisotropy may be obtained by injection moulding of STCPs.[19,20] The benefits of such an anisotropic microstructure is confirmed by a recent report of an anisotropic silicone valve, manufactured by additive manufacturing techniques.[21]

The estimated number of patients per year requiring heart valve replacements by 2050 is >1 million.[22] Being inexpensive, while combining durability and biocompatibility, a novel PHV could benefit young and elderly patients globally with a one type-fit-all approach.

Here we describe the design, development and testing of a novel PHV, named Poli-Valve,[23] manufactured by injection moulding of styrenic triblock copolymers with cylindrical microstructure. This cylindrical microstructure is formed by self-assembly resulting from the segregation of the styrenic and elastomeric blocks of the triblock copolymers: the cylinders are of well-defined diameter (order 10 nm) and spacing (order 20 nm), and having a high aspect ratio; the cylinders may be preferentially oriented by melt flow.[19] The new valve is entirely polymeric with only two structural components: leaflets and stent, made from different grades of the same material.

Haemocompatibility of a selection of styrenic block copolymers has previously been tested *in vitro* using a modified Chandler loop according to ISO 10993:4 and is reported elsewhere.[24] The work shows that styrenic block copolymers tested elicited no adverse host response in haemocompatibility or direct fibroblast contact. Measures of platelet and coagulation cascade activation indicated that the test materials were superior to polyester and similar to bovine pericardium reference materials. Inflammatory measures showed minimal haemolysis and immune system activation better than for polyester and bovine pericardium. Moreover, the addition of a heparin coating further reduced protein adsorption and improved *ex vivo* haemocompatibility performance in all measures. A similar block copolymer, SIBS, has also been shown to have low thrombogenic activity.[25,26]

Methods

PHV design, bench-based development and evaluations

Materials. In valve development we have used commercial block copolymers poly(styrene-*block*-ethylene/propylene-*block*-styrene) (SEPS) and poly(styrene-*block*-ethylene/butylene-*block*-styrene) (SEBS) manufactured by Kraton. Although their intended use is mainly in automotive, adhesives, compounding *etc*., they are pure synthetic materials, obtainable in many grades in the market. For the time being, the manufacturer does not provide them for use as permanent biomedical implants; however, there are a number of other medical applications, and we have established a collaboration with Kraton to explore the use of their polymers in heart valve prostheses. Synthesis of the block copolymers is well known[27] and an equivalent to the best performing commercial material could be purposely made for use in heart valves, should this be necessary.

Molecular characterisation of the block copolymers (Table 1) was evaluated by gel permeation chromatography (GPC) using triple detection on a Viscotek GPCmax VE2001

Table 1 Molecular characterisation of materials

Material	Composition	Molecular weight (g mol^{-1})	PI index	Styrene fraction (wt%)
SEPS22	Poly(styrene-*block*-ethylene/propylene-*block*-styrene)	71 697	1.038	19.2
SEBS29	Poly(styrene-*block*-ethylene/butylene-*block*-styrene)	74 837	1.061	28.4
SEBS20	Poly(styrene-*block*-ethylene/butylene-*block*-styrene)	111 327	1.072	19.6

GPC Solvent/Sample Module. The detectors used were: refractive index, viscosity and light scattering. Tetra-hydro-furan was the eluent (flow 1 ml min^{-1}) at a constant temperature of 24 °C. The detectors were calibrated with polystyrene standard Malvern PolyCal™ Std-PS99k. The values for the refractive index increment (d*n*/d*c*) used for the calculation were 0.185 ml g^{-1} for polystyrene and 0.072 ml g^{-1} for both ethylene-butylene and ethylene–propylene blocks.

Microstructure characterisation of the block copolymers and structural alignment in the heart valve leaflets was evaluated by Small Angle X-ray Diffraction using the Bruker Nanostar instrument.

Design, prototyping, relative costs and timing. Prototype designs were refined with the aid of computational modelling, fully described elsewhere.[18,28] Briefly, this resulted in development of a computational tool to optimize the alignment of cylindrical domains along directions of maximum stress, mimicking the alignment of collagen bundles in natural heart valve leaflets. This optimized alignment resulted in minimisation of strain energy density, which in turn is expected to maximise durability.

PHVs were manufactured by injection moulding. Briefly, the overall process cycle comprises the following steps: melting of block copolymer granules, injection into the mould cavity in the form of a viscoelastic polymer flow, packing, cooling, and removing of the moulded part. The method offers relatively inexpensive and highly reproducible manufacturing. The injection was achieved through a channel narrowing from diameter 2 mm to 0.4 mm, which minimised the size of the sprue. The reduction of the channel helped also to detach the sprue spontaneously, leaving only about 1 mm of excess material sticking out of the heart valve leaflet's surface.

In the process of prototyping, making of injection moulding tools is the most laborious and expensive stage, especially when the tools are made in stainless steel by commercial mould manufacturers, such as those used for the prototypes F and B (see Table 2).

In order to reduce costs and manufacturing time a new machining process was adapted from aerospace machining techniques used by the Whittle Laboratory at the University of Cambridge. These tools (Fig. 1A) are made in aluminium alloy and by five axis CNC machining. This allows shorter, stiffer cutters to be used to mill the mould which results in improved surface finish, accuracy, reduced machining cycle time and therefore lower cost. The decision to use the new process allowed more valve designs to be tested in the project. After preliminary mathematical modelling studies and initial prototype testing *ex vivo*, the design was further refined based on clinician feedback.

Prototype valves selected for animal trials, have been heparin coated using either Corline Heparin Conjugate CHC™ (Corline Biomedical AB, Sweden) or Astute® Advanced Heparin Coating (Biointeractions Ltd, UK). Finally, the valves have been sterilised with ethylene oxide shortly before the surgery.

Relative costing and timing necessary for valve production was assessed to inform the future financial case of our device toward clinical impact and commercialisation.

Durability. Durability of the PHV prototypes was assessed in an accelerated fatigue tester (TA Electroforce) at 30 Hz with water at 37 °C as the working fluid, under test conditions specified by ISO 5840:2015, which requires 100 mmHg pressure difference across the closed aortic valves for at least 5% of each cycle, and this should be maintained for more than 95% of all test cycles (Video 1, ESI†). The durability testing of the latest prototype J6 ($n = 4$) has taken 17 months to complete, which explains the relatively high testing frequency chosen. Valves were videoed under stroboscopic illumination in the accelerated fatigue tester, and the extent of opening at various frequencies could not be distinguished; the mean geometric orifice area expressed as a percentage of the mean geometric at 30 Hz (±standard deviation) measured using two different sample valves in two different testing chambers was 98% (±3%) at 25 Hz, 101% (±6%) at 20 Hz and 96% (±4%) at 15 Hz. Each valve was mounted in an independently controlled testing chamber, where removal or adjustment of one sample did not affect other samples. Valve failure was identified by abnormal proximal and distal pressure traces, followed by visual inspection. Durability test outcome for the earlier prototypes is reported for the following models: B ($n = 8$), F ($n = 11$), J1 ($n = 8$), J2 ($n = 8$), J3 ($n = 5$), J4 ($n = 3$) and J5 ($n = 11$).

Hydrodynamic performance. Hydrodynamic performance of the PHVs at the bench was evaluated in a pulse duplicator system according to methods described elsewhere.[23] Briefly, the pulse duplicator comprises of a volumetric pumping system, a ventricular chamber, an aortic valve housing, a three parameters systemic impedance simulator and a mitral valve housing. The pulse duplicator is able to reproduce the physiological stroke volume, pressure and flow waveforms of the left ventricle of the human heart. The PHVs were tested in the aortic position with a mechanical, tilting disc valve mounted in the mitral position with water at 20 °C as the working fluid. The test conditions conformed to ISO 5840:2015 requirements *i.e.* frequency of 70 bpm, simulated cardiac output 5 l min^{-1}, systolic duration 35% at normotensive conditions (Video 2, ESI†). Simultaneous flow and pressure measurements upstream and downstream from the aortic valve were recorded by using Transonic ultrasound flowmeters and pressure transducers, respectively. Bench-based hydrodynamic performance of each valve was evaluated, as per ISO 5840-2:2015, by calculating Effective Orifice Area (EOA) according to eqn (1), average systolic trans-valvular pressure drop (ΔP), and regurgitation fraction (REG).

$$\mathrm{EOA} = \frac{Q_{\mathrm{RMS}}}{51.6\sqrt{\frac{\Delta P}{\rho}}} \quad (1)$$

where the EOA is calculated in cm^2, Q_{RMS} is the root mean squared forward flow (ml s^{-1}) during the positive differential pressure period ($\Delta P > 0$), ΔP (mmHg) is the mean pressure difference (measured during the positive differential pressure

Table 2 Characteristics of successive (top to bottom) heart valve prototypes. Note that J5 and J6 are identical, except for leaflet thickness

Valve prototype	Single injection of SEPS22	Over-moulding SEBS20 on SEBS29 stent	Injection to leaflets free edge	Injection to leaflets centre	Spherical leaflets	Cylindrical leaflets	Fillet around leaflets	Adjusted leaflets profile	Nodules in the middle of free edge	Heparin coating	Mean leaflets thickness, mm	Limitations/mode of failure
B	X		X		X						0.26	Leaflets too thin, very short durability, failure at commissure
F	X		X		X		X				0.37	Poor hydrodynamics, uneven leaflets thickness leading to short durability/failure at commissure and the centre of the free edge
J1	X		X		X		X	X			0.36	Poor hydrodynamics, short durability/failure at the centre of the free edge
J2	X		X		X		X	X	X		0.36	No advance of nodules
J3	X		X		X		X	X		X	0.36	Too large posts, no fit to anatomy, short durability/failure at commissure
J4		X		X	X		X	X			0.35	Durability below min ISO 5840 requirements/failure at commissure
J5		X		X		X	X	X			0.22–0.48	Short durability for thin leaflets valves, poor hydrodynamics for thick leaflets valves/failure at commissure or free edge
J6		X		X		X	X	X			0.40	Failure at commissure or free edge

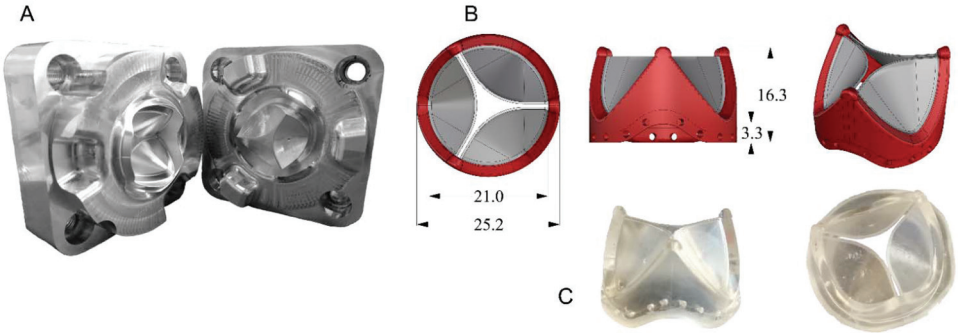

Fig. 1 Manufacturing of J6 PHV: (A) aluminium mould inserts for the J6 valve; (B) CAD design; (C) J6 valve with preformed suturing holes (left); and with "skirt" for clamping into *in vitro* testing equipment (right).

period), and ρ (g cm^{-3}) is the density of the test fluid. The evaluated regurgitant fraction included closing volume, transvalvular leakage volume and paravalvular leakage volume, and is expressed as a percentage of the forward flow volume. Comparisons were made between similar PHVs with differences in leaflet thickness and between the J5 (n = 6 for each thickness) and J6 (n = 13) prototypes *vs.* the best-in-class and most commonly used bio-prosthesis (BIC-B, n = 2), namely the Carpentier-Edwards Perimount Pericardial Bioprosthesis.

Haemocompatibility. Thrombus formation was assessed using the Badimon chamber, which records thrombogenicity of flowing blood in patients with coronary artery disease[29–31] and the efficacy of antithrombotic agents.[32–34]

For this study, 10 healthy subjects (demographic data see ESI Table S1†) with no known history of coronary artery disease, diabetes mellitus, haematological dyscrasias or on blood thinning medications were recruited.

In brief, a pump was used to draw blood from the antecubital vein through a series of three cylindrical perfusion chambers maintained at 37 °C in a water bath. The three perfusion chambers are arranged in series with blood flowing initially through the first, low shear and then the second and third high shear chambers. Strips of material, cut to fit inside the chambers, acted as the thrombogenic substrate. The rheologic conditions in the first chamber simulate those of patient coronary arteries (low shear rate, approximately 212 s^{-1}), whereas those in the second and third chambers simulate those of mildly stenosed coronary arteries (high shear rate, approximately 1690 s^{-1}). The model thus acts as one of deep coronary arterial injury. Each study lasted for 5 min, during which flow was maintained at a constant rate of 10 mL min^{-1}. All studies were performed using the same perfusion chamber and by the same operator. Immediately after each study, strips of material were removed and fixed in 4% paraformaldehyde.

Strips of thrombus laden polymer were fixed using 10% neutral buffered formalin without paraffin processing. The polymer material was not resistant to xylene which is used as a clearing reagent. Consequently, it was not possible to paraffin process the material which is our usual process when using porcine aorta.

Neutral buffered formalin was used as it resulted in less cracking of the clotted blood and better retention on the polymer when compared to test samples using 99% alcohol, then transferring directly to water-based staining reagents.

Test samples were stained with Masson Trichrome to identify fibrin.

Study samples were stained by adding staining reagents directly to the labelled pots containing the polymer, rather than affixing the polymer to slides. This was done to overcome the difficulty of handling the delicate polymer strips without damaging any affixed clotting material. The polymer was handled using forceps where necessary, and the polymer and pots were rinsed in running water between staining steps. The following staining steps were performed:

Chromium trioxide – 60 min
Bleach in sodium metabisulphite – 1 min
Weigerts haematoxylin – 15 min
Blue in Scott's tap water
Ponceau-acid fuchsin – 3 min
Differentiate in phosphomolybdic acid – 10–20 min
0.25% light green – 10–20 min

The samples were dehydrated in graded alcohols then air-dried, omitting the final xylene step. Once dry, the polymer was mounted on plain glass microscope slides using Pertex mountant and cover slipped.

Images were captured using an Olympus BX51 optical microscope with a Nikon DS-Fi2 microscope camera.

Preliminary clinical feasibility evaluations

Preliminary clinical feasibility evaluations consisted of *extra-vivo* (porcine/sheep hearts, animal cadavers), and *in vivo* (sheep) and bench-based evaluations. Extra-vivo refinement focused on shape, height/profile, external diameter, flexibility, and suturability (n = 8) and included prototypes J3, J4 and J6. Key goals were 1. To achieve the smallest possible external diameter at a given effective orifice area; 2. To obtain an elastic/flexible PHV able to follow *in vivo* the systolic-diastolic motion of the aortic annulus; 3. To achieve a fabric-free suturing system. In addition, we assessed the compatibility of the PHV with magnetic resonance imaging (MRI) and clinical steriliza-

tion techniques, which consisted of sterility testing and serial bench-based evaluations of durability and hydrodynamic performance with and without sterilisation (these results are reported in Table S2, ESI†). The *in vivo* preliminary safety/feasibility pilot study consisted of short-term basic evaluations assessing functional (echocardiography) and biocompatibility performance (PHV clotting at histopathology) of J6 prototype in a sheep model (n = 3) with recovery ranging from 1 hour (n = 2) to 24 hours (n = 1) after cardiac surgery with cardiopulmonary bypass (CPB) and cardioplegic arrest (CA), through left thoracotomy. The case to be recovered for 24 hours post-surgery was managed only with aspirin 300 mg day^{-1}. The rationale for this early feasibility study was to ensure safety by assessing *in vivo* function with a view to get clearance toward a subsequent long-term experimental trial.

The animal procedures were undertaken at the University of Bristol Translational Biomedical Research Centre (TBRC), a preclinical large animal facility operating at Home Office, Good Laboratory Practice and clinical healthcare standards. All procedures were approved by the University of Bristol Research Ethics committee and performed in accordance with the Guide for the Care and Use of Laboratory Animals and the United Kingdom Animal (Scientific Procedures) Act, 1986, under Home Office Project Licence PPL 7008975.

Results

PHV design and bench-based development and evaluations

Design, prototyping, relative costs and timing. A summary of the geometric and manufacturing features explored in development of our valve prototype is presented in Table 2. Precision mould machining required only one week from design to implementation, allowing the testing of a wide range of geometric features, giving iterative improvements to the performance of the prototype valves. Development was also informed by clinician/surgical feed-back. This development process led to the latest design J6 (Fig. 1B and C), which was the result of testing various leaflet shapes and heights, moulding methods and block copolymers to achieve a clinically effective PHV.

The J6 design is manufactured by over-moulding SEBS20 (containing 20 wt% styrene) leaflets onto a previously fabricated SEBS (containing 29 wt% styrene) stent and is the prototype taken into *in vivo* feasibility testing. Similarly to collagen fibre orientation in native heart valve tissue, the orientation of styrene cylinders in the PHV leaflets is crucial to the valve's performance.[18,35] The closest analogy to the microstructure of the native heart valve was achieved by polymer injection into the middle of each valve leaflet. The microstructure orientation for J6 leaflet is shown in Fig. 2.

The leaflet was X-ray scanned with 1 mm and 2 mm spatial interval in horizontal and vertical directions, respectively and the microstructure in Fig. 2 is represented by a vector graph, where the angle of the vectors corresponds to the actual orientation of the styrene cylinders and the length of the vectors is

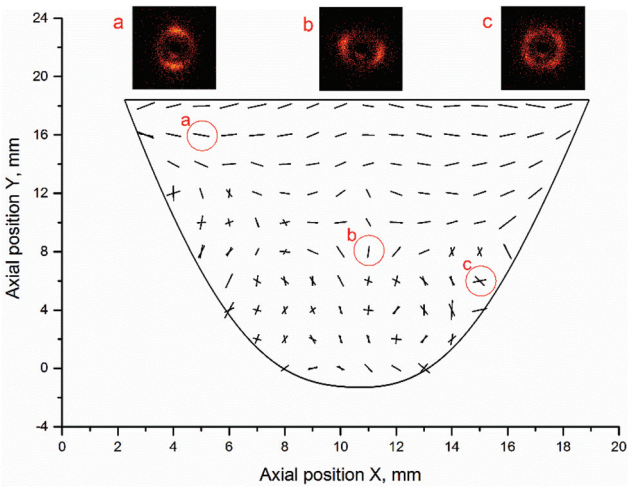

Fig. 2 A map of cylinder orientation within J6 valve and selected SAXS images showing the microstructure oriented (a) mostly horizontally, (b) mostly vertically and (c) cross-wise.

proportional to the azimuthal peak integral. The area above the injection point shows mostly circumferential orientation of cylinders, similar to collagen fibres orientation in the native heart valve tissue. Below the injection point a bi-modal orientation was formed, with part of the material aligned along the flow and part transverse to the flow direction. Formation of the bi-modal orientation by shear and extensional flow of the polymer melt in the mould, has been reported in detail elsewhere.[19] The ordering of the cylinders was enhanced by 10 minutes annealing of the polymer, taking place during slow mould cooling after the injection moulding. Such microstructure also exists in the natural heart valve leaflet tissue, where circumferentially arranged collagen fibres coexist with radially oriented elastin layer. The possibility of manufacturing materials, having such a bio-inspired microstructure, in one simple moulding process, is believed to be highly advantageous.

Due to the small size of the valve leaflets and complex distribution of orientation, we have not been able to directly correlate orientation with mechanical properties in the leaflets themselves. However, we have done extensive experimental[13–15,19,20] and modelling[18,35] work to demonstrate the relationship between orientation and mechanical properties (and so durability) on larger flat samples.

The cost of valve manufacture includes tools, polymer and coating, resulting in a modest manufacturing cost of £100 per valve or less. The aluminium moulds can be machined within 12 hours and can produce hundreds of parts. Injection moulding of the valve, cooling and valve extraction takes minutes. The speed, simplicity and inexpensiveness of manufacturing raise the intriguing future possibility of tailoring the detailed three dimensional shape of a valve to the individual patient, based on pre-operational imaging.

Durability. The durability of PHV prototypes was tested according to ISO standard 5840:2015; with marked improve-

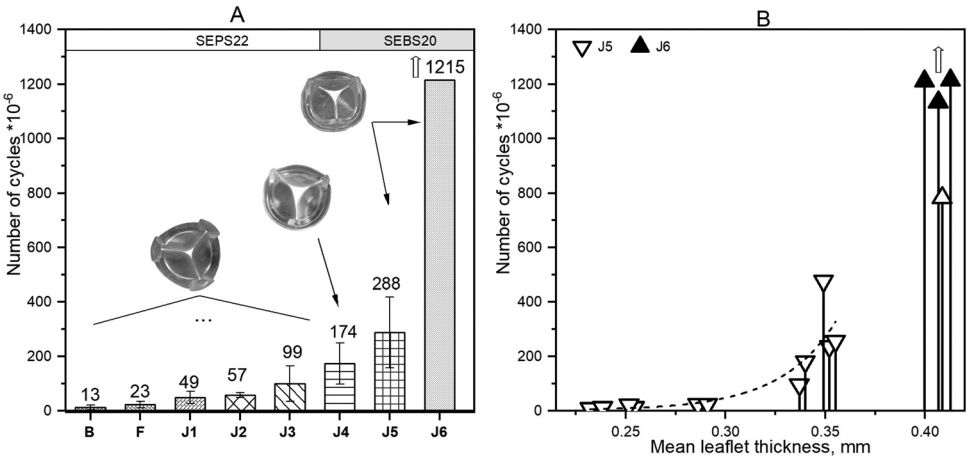

Fig. 3 Bench durability testing: (A) durability of PHV prototypes with leaflets made from SEPS22 and SEBS20. Error bars represent one standard deviation. Data for J6 valves does not show any variation and represents the actual state of ongoing test. (B) Durability as a function of mean leaflet thickness for J5/J6 design. Ongoing durability testing of the J6 prototype is shown by shaded markers, while finished tests are represented by unfilled markers.

ment of successive prototypes B to J6, from 13 million cycles to >1.2 billion ($p > 0.0001$) (Fig. 3A). Durability was also affected by the valve manufacturing process. Significant durability enhancements were achieved by using a softer leaflet material SEBS20 and shifting the injection point to the centre of the leaflet (prototypes J4–J6) from injection onto the free edge (prototypes B–J3).

Durability was strongly affected by leaflet thickness as shown by the number of cycles achieved in the accelerated tester for valves of the same design (J5 and J6) but with various leaflet thicknesses, shown in Fig. 3B, where J6 is the valve with optimised leaflet thickness.

The commonest failure mode of the J5 valves was formation of a vertical crack from a free edge of the leaflet through the injection point and down to the leaflet base. Some valves of this type also failed due to crack formations at the commissure.

Four valves of the latest prototype J6 (two 19 mm and two 21 mm ID) have been tested for durability. One of the 21 mm valves (v29) failed after 783 million cycles due to a vertical crack near the commissure in one of the leaflets. The leaflets of this valve also showed some minor defects at the free edge. The remaining valves have surpassed 1.1 billion (v50) and 1.2 billion cycles (v38 and v55) and are still going.

Hydrodynamic performance of each valve was measured before fatiguing and repeated after 500 million and then every 100 million cycles. The measurements of EOA and REG are presented in Fig. 4A and B, respectively. Beyond 500 million cycles the opening area decreased by 10–15% compared to before fatiguing; the EOA of the valves remained well above the minimum required by ISO standards (0.85 cm^2 for 19 mm and 1.05 cm^2 for 21 mm). The free edge of three of the valves (v29, v38 and v50) started to show some damage beyond 500 million cycles, resulting in a somewhat increased regurgitation fraction. One of the 21 mm valves (v38) started to regurgitate >10% at 600 million cycles and gradually worsened to 1.2 billion cycles. At 1 billion cycles one of the 19 mm valves (v50) also exceeded the 10% regurgitation limit specified by ISO standards for surgical valves and this continued at 1.1 billion cycles. Nevertheless after 1.1 billion (v50) and 1.2 billion cycles (v38) the regurgitation fraction was still smaller than 20%, which is the maximum allowed by ISO for trans-

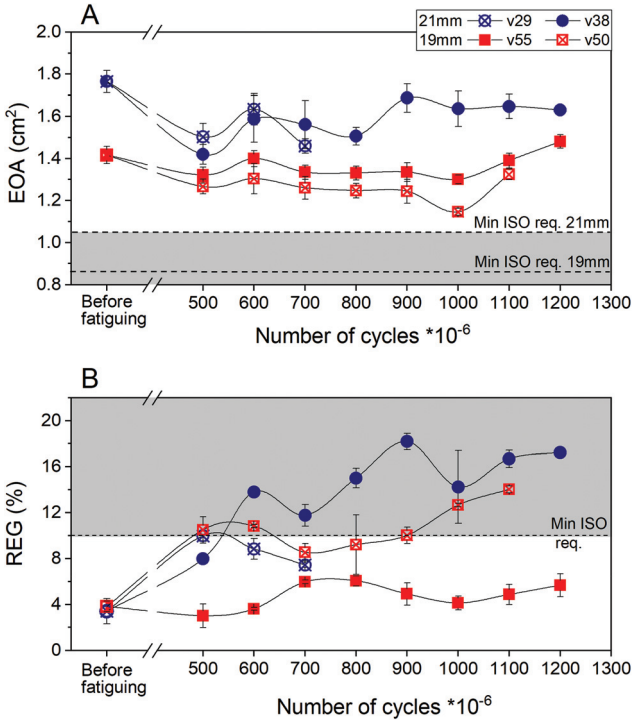

Fig. 4 Hydrodynamic performance of fatigued J6 valves. (A) Effective Orifice Area (EOA); (B) fractional regurgitation (REG). Error bars indicate variation between repeated measurements of the same valve.

catheter valves. It is thus anticipated that valves performing in this way would not significantly compromise the health of a patient, while having high potential to improve it. One of the 19 mm valves (v55) at 1.2 billion cycles remained fully functional as required by ISO (EOA = 1.48 cm^2, REG = 5.66%). Fatigue data for this test was collected for over 17 months at 30 Hz; 1.2 billion cycles are equivalent to over 30 years of operation at 72 bpm.

There is substantial variation in long term performance of the four J6 valves tested for durability (most notably one of the four failing after 783 million cycles). In general, it appears (although with only two samples of each) that the 19 mm diameter valves perform better than the 21 mm diameter ones. This is consistent with the 19 mm valves having, *pro rata*, slightly thicker leaflets than the 21 mm ones, a result of minor mould variability. However, substantial variability remains between notionally identical J6 valves of the same diameter; this is ascribed to minor variations in processing conditions during manufacture of each valve. Improved quality control to achieve optimal performance consistently for all valves manufactured is an essential part of future work towards clinical application.

Hydrodynamic performance (HP). A representative example of the pressure and flow waveforms acquired during the pulsatile test (5 l min^{-1}, 70 bpm) of our latest design (J6) valve is presented in Fig. 5B.

Fig. 5C–E shows the hydrodynamic performance of designs J5 and J6, which are geometrically identical with the exception of leaflet thickness. Five pairs of aluminium mould inserts were used to manufacture valves having average leaflets thickens of 0.24 mm, 0.30 mm, 0.35 mm, 0.40 mm and 0.46 mm, but otherwise identical geometry, so the effect of the thickness could be assessed independent of other factors. Six 21 mm valves of each thickness were tested in the pulse duplicator system. All valves exceeded minimum ISO standard requirements. Leaflet thickness markedly affected hydrodynamic performance, especially EOA, which reduced from 2.5 cm^2 to 1.1 cm^2 with increasing leaflet thickness from 0.24 mm to 0.46 mm (Fig. 5C). Mean pressure gradient ΔP also considerably increased (from 8 to 25 mmHg) as the thickness increased (Fig. 5E). Test data for REG was more scattered, due to occasional paravalvular leak in the valve housing system, but the general trend showed a drop in regurgitation fraction with increasing thickness of the leaflets (Fig. 5D).

Comparison of PHV *vs.* BIC-B. The measured hydrodynamic performance of the BIC-B (Carpentier-Edwards Perimount Pericardial Bioprosthesis) is also shown in Fig. 5C–E. The EOA and mean ΔP of the BIC-B are similar to those of the PHVs with leaflet thickness of 0.35–0.40 mm (coincidentally approximately the same as the thickness of the pericardium tissue making up the leaflets of the BIC-B).

Snapshots of the PHV and the BIC-B at peak diastole and systole are shown in Fig. 5A, allowing a comparison of the opening area at peak systole, as well as the shape of the fully open orifice for both polymeric (J6) and reference valves. The PHV showed a more circular opening and its geometrical opening area at peak systole was 15% larger than for the Perimount valve. The calculated mean values of EOA for the J6 21 mm PHV (*n*

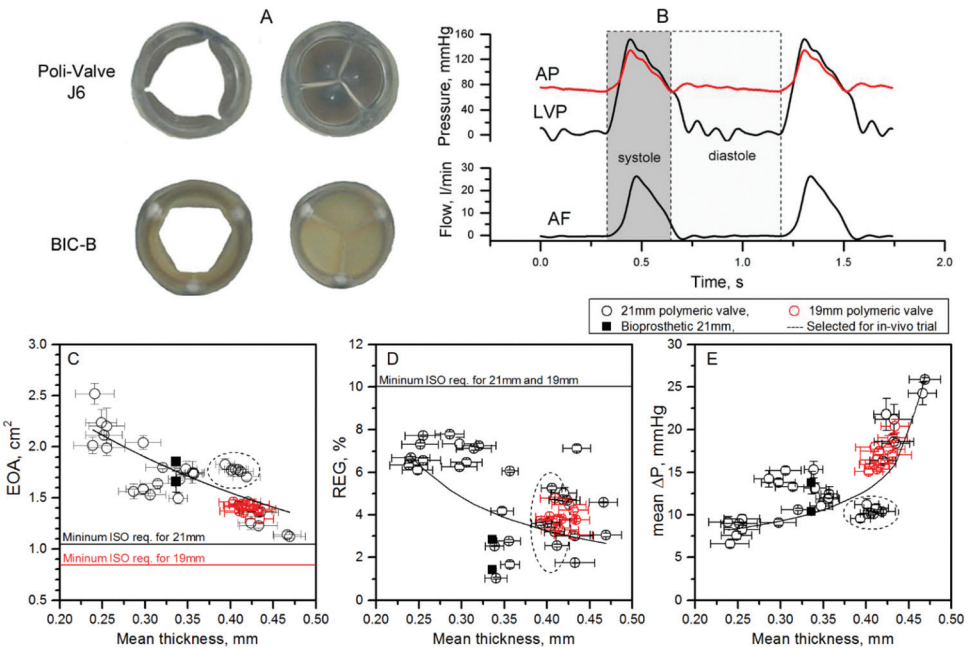

Fig. 5 Measurements of hydrodynamic performance: (A) prototype J6 21 mm and Edwards Perimount 21 mm valve at peak systole (left) and diastole (right); (B) pressure and flow waveforms acquired during pulsatile tests of J6 valve: AP is aortic pressure, LVP left ventricular pressure, and AF aortic flow; (C) Effective Orifice Area (EOA); (D) regurgitant fraction (REG); (E) mean systolic pressure gradient ΔP. Error bars represent one standard deviation. The trend line catches the effect of leaflet thickness on hydrodynamics of 21 mm polymeric valves. Results for the J6 valve (21 mm) are circled by a dashed line; the 19 mm J6 valve selected for *in vivo* testing is represented by red markers. All data are prior to fatiguing.

Table 3 Bench-based hydrodynamic performance of J6 valve

Valve	Qty	EOA (cm^2)	REG (%)	Mean ΔP (mmHg)	Max ΔP (mmHg)
Polymeric 19 mm	$n = 7$	1.42 ± 0.04	3.82 ± 0.47	16.19 ± 1.01	30.69 ± 1.74
Polymeric 21 mm	$n = 6$	1.77 ± 0.05	3.40 ± 1.10	10.41 ± 0.66	22.94 ± 1.33
Bioprosthetic 21 mm	$n = 2$	1.76 ± 0.13	2.13 ± 0.76	11.90 ± 1.87	23.68 ± 1.05

Values are shown as mean ± standard deviation.

= 6) was 1.77 ± 0.05 cm^2, which was almost the same as for the reference valve ($n = 2$) 1.76 ± 0.13 cm^2. The inconsistence between the geometrical and calculated opening area can be explained by different dynamics of opening for the two types of valve.

To guarantee good size-matching for the aortic annulus of a typical 70–80 kg adult sheep for preliminary *in vivo* short-term evaluations, two sizes of the J6 valve were prototyped: 21 mm and 19 mm internal diameter. The hydrodynamic performance of these two sizes of prototype J6, as well as the reference BIC-B 21 mm is shown in Table 3.

Haemocompatibility

The images from polymer samples treated in the Badimon chamber at high (1920 s^{-1}; Re 60) and low shear (500 s^{-1}; Re 30) (Fig. 6) did not show thrombus aggregation as typically seen when using porcine aorta as the thrombogenic substrate.[29–31] We were unable to perform quantitative analysis given the absence of thrombus. Qualitatively, a thin layer of fibrin and/or red blood cells were seen in the samples. The images shown are from heparin coated samples; uncoated samples were also tested, with similar results. Previous work has shown that heparin coating of similar block copolymers reduces the thrombogenicity of surfaces.[24] The Badimon chamber technique was not able to resolve this difference, but it did confirm that all samples (heparin coated and uncoated) showed good haemocompatibility.

The durability of heparin coating was assessed *in vitro*; in previous work[24] it was shown, by XPS monitoring of surface sulphur, to be stable over 500 hours in a variety of solutions, with or without dynamic strain. Only a strongly oxidising solution (3% aqueous H_2O_2) resulted in rapid loss of surface coating. Using the same XPS technique, we have shown that a heparin coated valve retains 60% of its surface sulphur after 190 million cycles (4.5 years equivalent) in the accelerated fatigue tester.

Preliminary clinical feasibility evaluations

Extra-vivo developmental/feasibility evaluations. Extra-vivo refinement of the PHV focused on 3D shape, low profile, external diameter, flexibility/elasticity and suturability: findings from representative experiments are shown in Fig. 7A–C. We undertook a series of surgical implantations and size-matching procedures ($n = 8$) on pre-sized aortic annulus in porcine

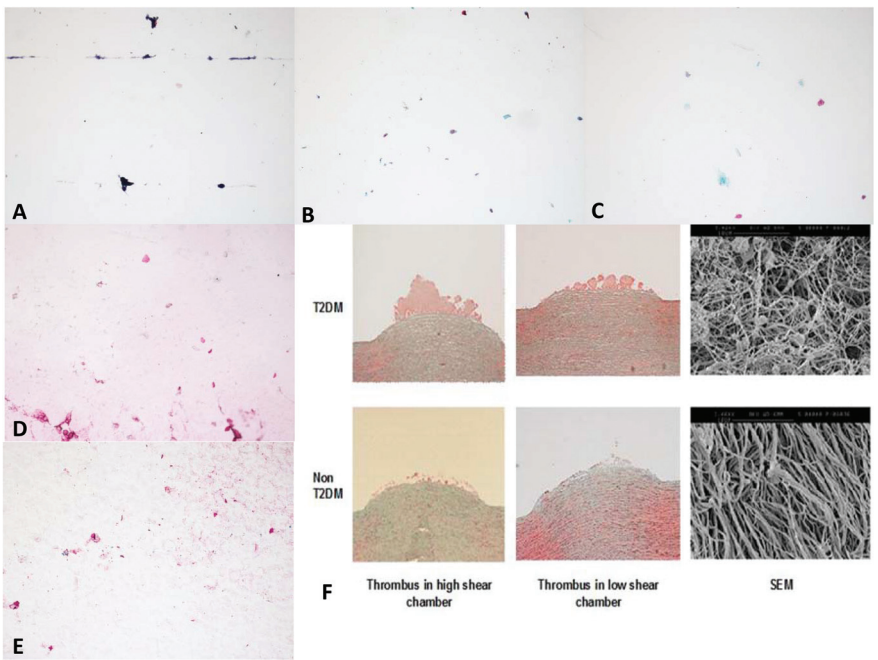

Fig. 6 Images taken from samples treated in the Badimon chamber: (A) a heparin coated (Corline) sample placed in a high shear chamber showing no thrombus; (B) a heparin coated (Corline) sample placed in a low shear chamber showing small clumps of red blood cells and fibrin; (C) a heparin coated (Corline) sample placed in a high shear chamber showing small clumps of red blood cells and some fibrin staining; (D) a heparin coated sample (Biointeractions) placed in a high shear chamber showing red blood cells and fibrin; (E) a heparin coated sample (Biointeractions) placed in a low shear chamber showing red blood cells and fibrin; (F) images from earlier experiments[31] showing thrombus formation over porcine aorta stripped of intima (SEM = scanning electron microscopy). Optical images were taken at ×10 magnification, SEM at ×100 000.

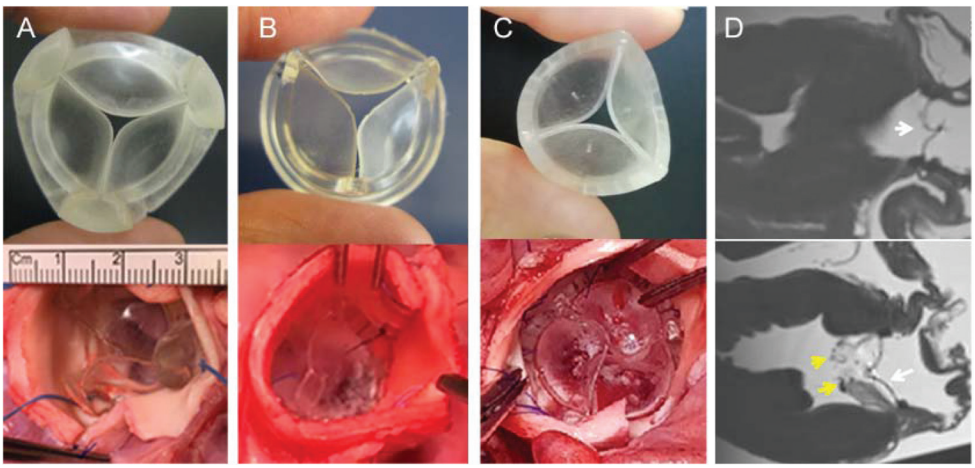

Fig. 7 Representative illustrations of PHV prototypes during development (upper panels) and aligned extra-vivo procedures (lower panels): (A) prototype J3; (B) prototype J4; (C) prototype J6; (D) MRI compatibility: longitudinal view of PHV sutured in aortic position (upper panel, white arrow) and mitral position (lower panel, white arrow); note native mitral leaflets (yellow arrows) for imaging comparison with PHV.

hearts/cadavers, informing the changes implemented from PHVs prototype J3 (Fig. 7A) then J4 (Fig. 7B), to prototype J6 (Fig. 7C). The external diameter of a typical PHV with an internal diameter of 21 mm was reduced from 32 mm to 25 mm (Fig. 7A *vs.* 7C). The base shape changed from 2D flat to 3D saddle-shape to reflect the 3D lining of the porcine/human aortic valve annulus, while the height/profile was reduced to 13 mm (Fig. 1B). The consistency of the PHV changed from rigid/semi-rigid to flexible/elastic (see Video 3; ESI†) to reflect the need to preserve the physiologic dynamics of the native valvular annulus after implant. A fabric-free valve suturing system was achieved, based on 12–14 pairs of holes (0.5 mm diameter) as shown in Fig. 1B and C, which allowed excellent extra-vivo implantation of J6 (n = 4) without deformation (Fig. 7C).

Extra-vivo compatibility to magnetic resonance imaging (MRI) was assessed by suturing two PHVs in two porcine hearts in aortic (Fig. 7D upper) and mitral positions (Fig. 7D lower). The PHV inserted in the mitral position was intentionally sutured over the native mitral valve to allow direct comparative imaging evaluations with the native leaflets. This experiment showed excellent MRI compatibility of the PHV, and allowed a detailed morphological assessment of the PHV with no artefacts. Finally, the compatibility of the PHV with clinical sterilisation techniques was assessed by bench based evaluation with and without sterilisation, and the durability and hydrodynamic performance of the sterilised PHV was not adversely affected (data provided in ESI, Table S2†).

***In vivo* short-term feasibility evaluation.** The *in vivo* short-term feasibility study was carried out in 75–80 kg sheep in a model of cardiac surgery with CPB and CA through left thoracotomy (n = 3) with a recovery time ranging from 1 (n = 2) to 24 hours (n = 1). In all cases a 19 mm J6 PHV was inserted in supra-annular fashion using 4-0 prolene sutures (Fig. 8A). *In vivo* echocardiographic evaluations (n = 3) were recorded at 1 hour post-surgery, with an ongoing average systolic blood pressure of 96 ± 8 mmHg. There was no evidence of any perivalvular or trans-valvular regurgitation as seen in Fig. 8B (and Videos 4 and 5, ESI†). Measurements of the average trans-valvular peak gradient (Fig. 8C) indicated 23 ± 3 mmHg, in keeping with the bench-based hydrodynamic performance of the 19 mm J6 PHV. One of these 3 animals was kept for 24 hours after completion of surgery and extubated successfully for post-extubation safety assessment of short-term valvular integrity and biocompatibility. This animal was not anticoagulated and received only Aspirin 300 mg day^{-1}. Post-mortem confirmed intact structure of the PHV with no evidence of any acute valvular clot/thrombus.

Discussion

This study has several key findings. It shows that it is possible to use styrenic block copolymers to make a PHV as an alternative to mechanical and biological prostheses. PHV development required the implementation of refinements in design based on computational modelling (reported previously),[18] *in vitro* testing and clinician/surgical feedback, leading to successive prototypes manufactured by a highly reproducible (and inexpensive) injection moulding technique. The most recent PHV J6 prototype markedly exceeds the ISO standards in terms of hydrodynamic performance and durability. PHV J6 underwent *in vivo* preliminary short-term feasibility testing with very encouraging safety, functional and biocompatibility outcomes, supporting its progression into an experimental randomised trial, which has just started.

Inspired by the native valve, in which collagen fibres are aligned to bear stresses during loading, we utilised oriented styrene cylinders in block copolymers to reinforce the polymeric leaflets. Mechanical properties of the materials can be tailored by controlling microstructural alignment, which strongly depends on flow direction within the mould.

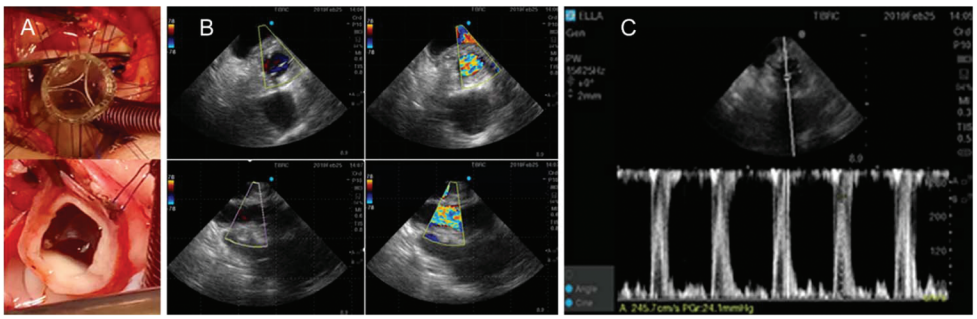

Fig. 8 Representative *in vivo* feasibility experiment using a J6 19 mm PHV with animal recovered and kept for 24 hours post-surgery: (A) PHV during (top) and after (bottom) suturing in aortic position; (B) end-diastolic echo-Doppler at 1 hour post-surgery showing no trans-valvular or peri-valvular jets in transverse (top left) and longitudinal (bottom left) views; end-systolic echo Doppler at 1 hour post-surgery showing blood flow across the opened PHV in transverse (top right) and longitudinal (bottom right) views; (C) measurement of transvalvular peak gradient (24 mmHg in this case) at the same time point.

Mapping of cylinders' orientation within leaflets of J6 revealed orientation of cylinders similar to the orientation of collagen fibres in native heart valve tissue.[13,14] Our finite element modelling, previously reported, demonstrates the importance and advantages of well controlled anisotropy *versus* anisotropic polymer,[18] with the former showing smaller strain and smaller strain energy density, which is directly related to durability. Experimental comparison of oriented and isotropic heart valve leaflets using accelerated fatigue tester was not possible, because it is very difficult to obtain isotropic samples using our manufacturing method. Moreover the performance of the valve results not only from the leaflet material microstructure but also from optimisation of its geometry and properties of its components. The microstructure orientation present in J6 has the closest analogy to the native heart valve anisotropy of all our prototypes.

The excellent bench durability achieved with the J6 prototype is also the result of progressive refinements (Fig. 3A). The early PHV prototypes showed insufficient durability (whilst achieving good hydrodynamic performance) with leaflet tears developing within a few tens of millions of cycles. We learned that PHV durability is not only a function of the polymer selected for leaflet construction, but is also highly dependent on valve design and manufacturing process. For example, it was enhanced by using a leaflet material (SEBS20) with better fatigue properties and by shifting the injection point to the centre of the leaflet instead of the free edge (prototypes B–J3). In addition, leaflet thickness was shown to be a critical parameter affecting both durability and hydrodynamic performance. Indeed, the number of cycles achieved in the accelerated tester for PHVs of the same design (J5 and J6) but with various leaflet thicknesses increased significantly with increasing leaflet thickness. Unsurprisingly, whilst thicker leaflets performed better in terms of durability, their opening area and transvalvular pressure gradient worsened (Fig. 6C and E). The best performing prototype J6 has a design capturing the optimal balance between these two key design requirements. In on-going durability testing, three of four J6 valves begin to show free edge fracture above 500 million cycles resulting in increased regurgitation, although all remain functional. Further geometrical optimisation of leaflets height, coaptation and thickness near the fee edge, is likely to improve the free edge resistance to damage. Nevertheless, the durability already achieved greatly exceeds the ISO requirement, which is 200 million cycles.

Calcification can be an important contributor to valve degeneration *in vivo* and its molecular mechanisms are difficult to reproduce *in vitro*. However, a recent study shows that a styrenic block copolymer is significantly less prone to calcification *in vitro* than is a polyurethane valve.[36]

Hydrodynamic testing is subject to considerable variation depending on the details of geometry and testing conditions used, *i.e.* the same valve can give different results when tested in different pulse duplicators under ostensibly similar conditions; for example the shape and flexibility of the outflow pipe affect the EOA measured.[37] For this reason, the hydrodynamic testing was compared to identical tests in the same equipment performed on the BIC-B of nominal diameter 21 mm (measured internal diameter 20 mm, measured external sewing ring diameter 29 mm), which is commonly considered a gold standard reference valve. Of note, the Edwards Perimount, which we used as BIC-B, showed slightly lower (although within the error bars) REG fraction (2.13 ± 0.76%) than the J6 PHV prototype (3.40 ± 1.10%), well below 10%, the ISO requirement for a 21 mm valve. Our bench-based results for the Edwards Perimount valve are similar to those reported by others for the same valve tested *in vitro*[38,39] and *in vivo*.[40,41]

Based on these experimental bench-test results, supported by structural FEM modelling (reported elsewhere[18]), leaflet thickness of 0.4 mm (prototype J6) was selected for feasibility short-term evaluation in a sheep model of cardiac surgery.

Extra-vivo clinical testing was of great value during the development process in picking up limitations of the early prototypes and suggesting refinements to the design to improve the external diameter, 3D shape, profile, flexibility/elasticity, suturability and handling, while checking the compatibility to MRI imaging and clinical sterilisation. In addition, the preliminary *in vivo* short-term testing confirmed basic functional

safety/feasibility on the J6 prototype in terms of early hydrodynamic performance (n = 3, echocardiography at 1 hours post-surgery) and biocompatibility (n = 1, post-mortem evaluation at 24 hours post-surgery). We used only 19 mm PHVs as this size is the smallest generally used in adult cardiac surgery, whilst in our *in vivo* model the aortic annulus/root of the 75–80 kg sheep used would not take a larger PHV without root enlargement. As a result of this positive safety/feasibility pilot study we are progressing into an experimental trial assessing the long-term performance of our PHV. This trial involves implantation into adult sheep recovered for six months with a focus on valve *in vivo* biocompatibility, haemodynamics, durability and susceptibility to calcification.

For the single *in vivo* experiment focusing on early biocompatibility/thrombosis the animal was kept for 24 hours after surgery on 300 mg of Aspirin per day without anticoagulation. Histopathology confirmed an intact PHV with no clots/thrombus at 24 hours, suggesting good short-term biocompatibility. This is in keeping with our observations *in vitro* where no thrombus collection was observed in either the heparin coated or the uncoated samples and as such, no quantification of thrombus amount was possible. Whilst the standard flow rate through the chamber was 10 mL per minute of blood for 5 minutes, it is reassuring to note that compared to porcine aorta (intima stripped) there were no thrombus clumps seen in any of the samples.

The work reported in this paper relates to development of a surgical valve. However much of what has been learnt can be transferred directly into a trans-catheter device, which we are at present in the early stages of developing, incorporating identical leaflets to the surgical valve.

Conclusions

A PHV valve has been developed and tested *in vitro*, and in a short-term *in vivo* study. The final prototype is an overmoulded composite of a stiffer support structure (made of SEBS29) and softer leaflets (made of SEBS20), incorporating cylindrically shaped leaflets with a concave leading edge profile. This is performing excellently, well beyond ISO 5840:2015 standards for *in vitro* performance and equivalent to the same diameter Edwards Perimount Bioprosthetic valve in hydrodynamic performance, with durability in excess of 1.2 billion cycles, equivalent to 30 years of operation. In addition, the prototype has passed preliminary feasibility *in vivo* short-term testing with very good haemodynamic and biocompatibility performance.

Abbreviations

PHV	Prosthetic heart valve
STCP	Styrenic triblock copolymer
SEPS	Poly(styrene-*block*-ethylene/propylene-*block*-styrene)
SEBS	Poly(styrene-*block*-ethylene/butylene-*block*-styrene)
BIC-B	Best-in-class bio-prosthesis (Carpentier-Edwards Perimount Pericardial Bioprosthesis)
SEBS20	SEBS having 20 wt% styrene content
SEBS29	SEBS having 29 wt% styrene content

Funding

This work was supported by the British Heart Foundation [grant SP/15/5/31548]. RA acknowledges support from the National Institute of Health Research Bristol Biomedical Research Centre, the British Heart Foundation [grant IG/14/2/30991], and Medical Research Council [grant MR/L012723/1]. GM acknowledges support from a Royal Academy of Engineering/Leverhulme Trust Senior Research Fellowship and King's College, Cambridge. EB acknowledges support from the Sydney Brenner/Du Pont studentship at King's College, Cambridge.

Conflicts of interest

JS and GDM are authors on patent US2017014546-A1. JS, MS, EB, GDM and RA have UK Patent Application 1902717.6 pending.

Acknowledgements

Dr Graham Christie (University of Cambridge) for performing microbiological tests; the veterinary anaesthetists, research nurses, lab technicians, perfusionists, and the animal interface technicians at the University of Bristol Translational Biomedical Research Centre. This work was supported by the MRC/ESPRC Newcastle Molecular Pathology Node.

References

1 K. M. Kim, F. Shannon, G. Paone, S. Lall, S. Batra, T. Boeve, A. DeLucia, H. J. Patel, P. F. Theurer, C. He, M. J. Clark, I. Sultan, G. M. Deeb and R. L. Prager, Evolving trends in aortic valve replacement: A statewide experience, *J. Card. Surg.*, 2018, **33**, 424–430.
2 M. B. Leon, T. M. Nazif and V. Bapat, Interpreting National Trends in Aortic Valve Replacement Let the Buyer Beware, *JACC*, 2018, **71**, 1628–1630.
3 S. J. Head, M. Òªelik and A. P. Kappetein, Mechanical versus bioprosthetic aortic valve replacement, *Eur. Heart J.*, 2017, **38**, 2183–2191.
4 R. Fareed Siddiqui, J. R. Abraham and J. Butany, Bioprosthetic heart valves: modes of failure, *Histopathology*, 2009, **55**, 135–144.
5 T. Rodriguez-Gabella, P. Voisine, R. Puri, P. Pibarot and J. Rodés-Cabau, Aortic Bioprosthetic Valve Durability Incidence, Mechanisms, Predictors, and Management of

Surgical and Transcatheter Valve Degeneration, *J. Am. Coll. Cardiol.*, 2017, **70**, 1013–1028.

6 D. Poli, E. Antonucci, V. Pengo, L. Migliaccio, S. Testad, C. Lodigianie, R. Facchinetti, G. Serricchio, P. Falco, C. Mangione, S. Masottini, L. Ruocco, R. De Caterina and G. Palareti, Mechanical prosthetic heart valves: Quality of anticoagulation and thromboembolic risk. The observational multicentre PLECTUM study, *Int. J. Cardiol.*, 2018, **267**, 68–73.

7 D. Bezuidenhout, D. F. Williams and P. Zilla, Polymeric heart valves for surgical implantation, catheter-based technologies and heart assist devices, *Biomaterials*, 2015, **36**, 6–25.

8 R. L. Lia, J. Russ, C. Paschalides, G. Ferrari, H. Waisman, J. W. Kysara and K. David, Mechanical considerations for polymeric heart valve development: Biomechanics, materials, design and manufacturing, *Biomaterials*, 2019, **225**, 119493.

9 B. Rahmani, S. Tzamtzis, R. Sheridan, M. J. Mullen, J. Yap, A. M. Seifalian and G. Burriesci, A new transcatheter heart valve concept (the TRISKELE): feasibility in an acute preclinical model, *EuroIntervention*, 2016, **12**, 901–908.

10 J. Scherman, D. Bezuidenhout, C. Ofoegbu, D. F. Williams and P. Zilla, TAVI for low to middle income countries, *Eur. Heart J.*, 2017, **38**, 1182–1184.

11 L. Pinchuk, G. J. Wilson, J. J. Barry, R. T. Schoephoerster, J. M. Parel and J. P. Kennedy, Medical applications of poly (styrene-block-isobutylene-block-styrene) ("SIBS"), *Biomaterials*, 2008, **29**, 448–460.

12 J. Brubert and G. D. Moggridge, Material selection and performance index for polymeric prosthetic heart valve design", *J. Med. Device*, 2015, **9**, 020912.

13 J. Stasiak, A. M. Squires, V. Castellato, I. W. Hamley and G. D. Moggridge, Effect of stretching on the structure of cylinder- and sphere- forming styrene-isoprene-styrene block copolymers, *Macromolecules*, 2009, **42**, 5256–5265.

14 J. Stasiak, A. Zaffora, M. L. Costantino, A. Pandolfi and G. D. Moggridge, Engineering orientation in block copolymers for application to prosthetic heart valves, *Funct. Mater. Lett.*, 2010, **3**, 249–252.

15 J. Stasiak, A. Zaffora, M. L. Costantino and G. D. Moggridge, A real time SAXS study of oriented block copolymers during fast cyclical deformation with potential application for prosthetic heart valves, *Soft Matter*, 2011, **7**(24), 11475–11482.

16 H. J. Sauren, W. Kuijpers, A. A. Van Steenhoven and F. E. Veldpaus, Aortic valve histology and its relation with mechanics – preliminary report, *J. Biomech.*, 1982, **13**, 97–104.

17 J. A. Stella and M. S. Sacks, On the biaxial mechanical properties of the layers of the aortic valve leaflet, *J. Biomech. Eng.*, 2007, **129**, 757–766.

18 M. Serrani, J. Brubert, J. Stasiak, F. De Gaetano, A. Zaffora, M. L. Costantino and G. D. Moggridge, A computational tool for the microstructure optimization of a polymeric heart valve prosthesis, *J. Biomech. Eng.*, 2016, **138**, 061001.

19 J. Stasiak, J. Brubert, M. Serrani, S. Nair, F. de Gaetano, M. L. Costantino and G. D. Moggridge, A bio-inspired microstructure induced by slow injection moulding of cylindrical block copolymers, *Soft Matter*, 2014, **10**, 6077–6086.

20 J. Stasiak, J. Brubert, M. Serrani, A. Talhat, F. De Gaetano, M. L. Costantino and G. D. Moggridge, Structural changes of block copolymers with bimodal orientation under fast cyclical stretching as observed by synchrotron SAXS, *Soft Matter*, 2015, **11**, 3271–3278.

21 F. B. Coulter, M. Schaffner, J. A. Faber, A. Rafsanjani, R. Smith, H. Appa, P. Zilla, D. Bezuidenhout and A. R. Studart, Bioinspired Heart Valve Prosthesis Made by Silicone Additive Manufacturing, *Matter*, 2019, **1**, 266–279.

22 P. Zilla, J. Brink, P. Human and D. Bezuidenhout, Prosthetic heart valves: Catering for the few, *Biomaterials*, 2008, **29**, 385–406.

23 F. De Gaetano, M. Serrani, P. Bagnoli, J. Brubert, J. Stasiak, G. D. Moggridge and M. L. Costantino, Fluid Dynamic Performances of a New Polymeric Heart Valve Prototype (Poli-Valve) tested under Continuous and Pulsatile Flow Conditions, *Int. J. Artif. Organs*, 2015, **38**, 600–606.

24 J. Brubert, S. Krajewski, H. P. Wendel, S. Nair, J. Stasiak and G. D. Moggridge, Hemocompatibility of styrenic block copolymers for use in prosthetic heart valves, *J. Mater. Sci. Mater. Med.*, 2016, **27**(32), 1–12.

25 J. Sheriff, T. E. Claiborne, P. L. Tran, R. Kothadia, S. George, Y. P. Kato, L. Pinchuk, M. J. Slepian and D. Bluestein, Physical Characterization and Platelet Interactions under Shear Flows of a Novel Thermoset Polyisobutylene-based Co-polymer, *ACS Appl. Mater. Interfaces*, 2015, **7**(39), 22058–22066.

26 T. E. Claiborne, G. Girdhar, S. Gallocher-Lowe, J. Sheriff, Y. P. Kato, L. Pinchuk, R. T. Schoephoerster, J. Jesty and D. Bluestein, Thrombogenic Potential of Innovia Polymer Valves versus Carpentier-Edwards Perimount Magna Aortic Bioprosthetic Valves, *ASAIO J.*, 2011, **57**, 26–31.

27 F. Lin, C. Wu and D. Cui, Synthesis and Characterization of Crystalline Styrene-b-(Ethylene-co-Butylene)-b-Styrene Triblock Copolymers, *J. Polym. Sci., Part A: Polym. Chem.*, 2017, **55**, 1243–1249.

28 G. Luraghi, W. Wu, F. De Gaetano, J. F. R. Matas, G. D. Moggridge, M. Serrani, J. Stasiak, M. L. Costantino and F. Migliavacca, Evaluation of an aortic valve prosthesis: Fluid-structure interaction or structural simulation?, *J. Biomech.*, 2017, **58**, 45–51.

29 K. Balasubramaniam, G. Viswanathan, R. Hardy, S. Marshall, A. Zaman and S. Razwi, Blood thrombogenicity is independently associated with serum TSH levels in post non ST elevation acute coronary syndrome, *J. Clin. Endocrinol. Metab.*, 2014, **99**(6), E1050–E1054.

30 G. Viswanathan, S. Marshall, K. Balasubramaniam, J. J. Badimon and A. Zaman, Differences in thrombus structure and kinetics in patients with type 2 diabetes mellitus

after non ST elevation acute coronary syndrome, *Thromb. Res.*, 2014, **133**(5), 880–885.

31 K. Balasubramaniam, G. Viswanathan, J. Dragone, R. Grose-Hodge, P. Martin, S. Troy, P. Preston and A. Zaman, Antithrombotic properties of rafigrelide: a phase 1, open-label, non-randomised, single-sequence, crossover study, *Thromb. Haemostasis*, 2014, **112**(1), 205–215.

32 K. Wahlander, M. Eriksson-Lepkowska, P. Nystrom, U. G. Eriksson, T. C. Sarich, J. J. Badimon, I. Kalies, M. Elg and A. Bylock, Antithrombotic effects of ximelagatran plus acetylsalicylic acid (ASA) and clopidogrel plus ASA in a human ex vivo arterial thrombosis model, *Thromb. Haemostasis*, 2006, **95**, 447–453.

33 M. U. Zafar, M. E. Farkouh, J. Osende, D. Shimbo, S. Palencia, J. Crook, R. Leadley, V. Fuster and J. H. Chesebro, Potent arterial antithrombotic effect of direct factor-Xa inhibition with ZK-807834 administered to coronary artery disease patients, *Thromb. Haemostasis*, 2007, **97**, 487–492.

34 M. U. Zafar, D. A. Vorchheimer, J. Gaztanaga, M. Velez, D. Yadegar, P. R. Moreno, S. Kunitada, J. Pagan, V. Fuster and J. J. Badimon, Antithrombotic effects of factor Xa inhibition with DU-176b: phase-I study of an oral, direct factor Xa inhibitor using an *ex vivo* flow chamber, *Thromb. Haemostasis*, 2007, **98**, 883–888.

35 A. Zaffora, J. Stasiak, A. Pandolfi, R. Fumero, G. D. Moggridge and M. L. Costantino, Improvement of static performances of biomorphic polymeric heart valve prostheses by tailoring the material orientation, *Int. J. Artif. Organs*, 2011, **34**(8), 706.

36 N. C. Kekec, M. B. Akolpoglu, U. Bozuyuk, S. Kizilel, N. Nugay, T. Nugay and J. P. Kennedy, Calcification resistance of polyisobutylene and polyisobutylene-based materials, *Polym. Adv. Technol.*, 2019, **30**, 1836–1846.

37 S. M. Retta, J. Kepner, S. Marquez, B. A. Herman, M. C. S. Shu and L. W. Grossman, *In vitro* Pulsatile Flow Measurement in Prosthetic Heart Valves: An Inter-Laboratory Comparison, *J. Heart Valve Dis.*, 2017, **26**, 72–80.

38 G. Tasca, R. Vismara, G. B. Fiore, A. Mangini, C. Romagnoni, S. Pelenghi, C. Antona, A. Redaelli and A. Gamba, Fluid-dynamic results of in vitro comparison of four pericardial bioprostheses implanted in small porcine aortic roots, *Eur. J. Cardiothorac. Surg.*, 2015, **47**, e62–e67.

39 S. Marquez, R. T. Hon and A. P. Yoganathan, Comparative Hydrodynamic Evaluation of Bioprosthetic Heart Valves, *J. Heart Valve Dis.*, 2001, **10**, 802–811.

40 G. Gerosa, V. Tarzia, G. Rizzoli and T. Bottio, Small aortic annulus: The hydrodynamic performances of 5 commercially available tissue valves, *J. Thorac. Cardiovasc. Surg.*, 2006, **131**, 1058–1064.

41 H. Okamura, A. Yamaguchi, T. Yoshizaki, H. Nagano, S. Itoh, H. Morita and K. Nai, Clinical Outcomes and Hemodynamics of the 19 mm Perimount Magna Bioprosthesis in an Aortic Position – Comparison With the 19 mm Medtronic Mosaic Ultra Valve, *Circulation*, 2012, **76**, 102–108.

